Supporting Information

Staphylococcus aureus glucose-induced biofilm accessory protein A (GbaA) is a monothiol-dependent electrophile sensor

Abhinaba Ray[§], Katherine A. Edmonds[§], Lauren D. Palmer[∞], Eric P. Skaar[∞] and David P. Giedroc[§,¶*]

[§]Department of Chemistry, Indiana University, Bloomington, IN 47405-7102 United States

[∞]Department of Pathology, Microbiology, and Immunology and Vanderbilt Institute for Infection, Immunology, and Inflammation, Vanderbilt University Medical Center, Nashville, TN, 37232 United States

[¶]Department of Molecular and Cellular Biochemistry, Indiana University, Bloomington, IN 47405-7102 United States

*Email: giedroc@indiana.edu

This Supporting Information file contains Supplementary Figures S1-S11, Supplementary Tables S1-S3 and *Supplementary References*.

Figure S1

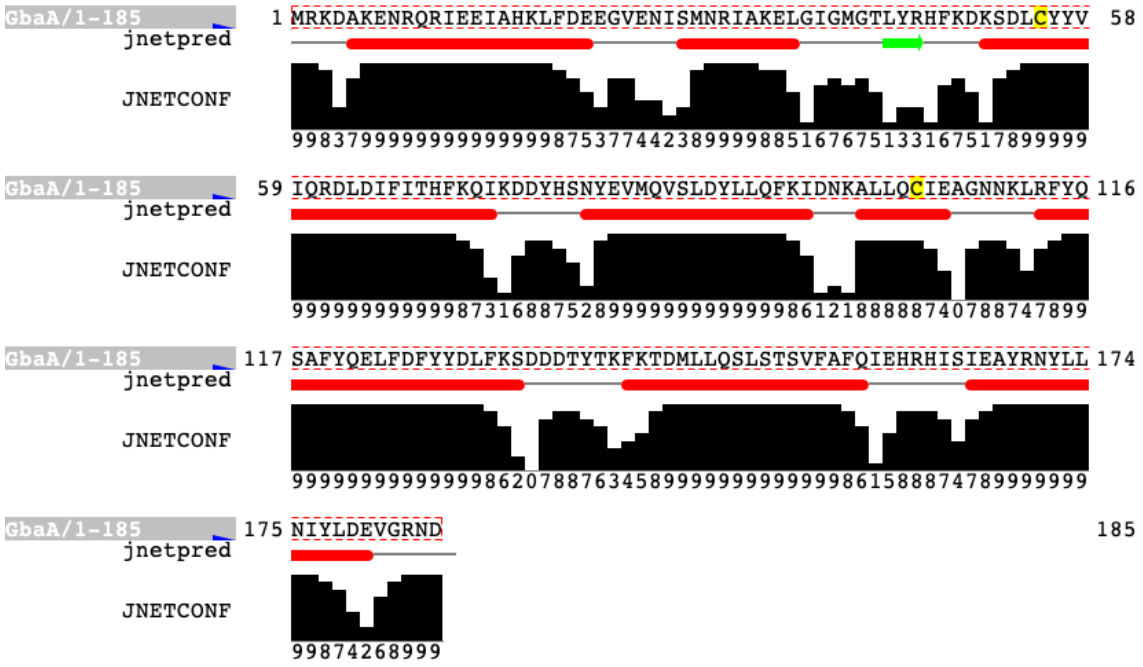

Figure S1. Secondary structure prediction of *S. aureus* GbaA obtained using Jpred4 webserver (http://www.compbio.dundee.ac.uk/jpred4) reveals a canonical TetR secondary structure (8 or 9 α-helices). The cysteine residues in the sequence are highlighted in *yellow*. Predicted α–helices are represented by the *red* bars and β–sheets by the *green* arrow. JNETCONF, confidence of assigning a particular amino acid to the indicated secondary structure (9, high; 0, low). Cys55 is present in the third α–helix in the N-terminal DNA binding domain (α1-α3), while Cys104 is present in the C-terminal domain, typically taken as the regulatory domain (α4-α8).

Figure S2

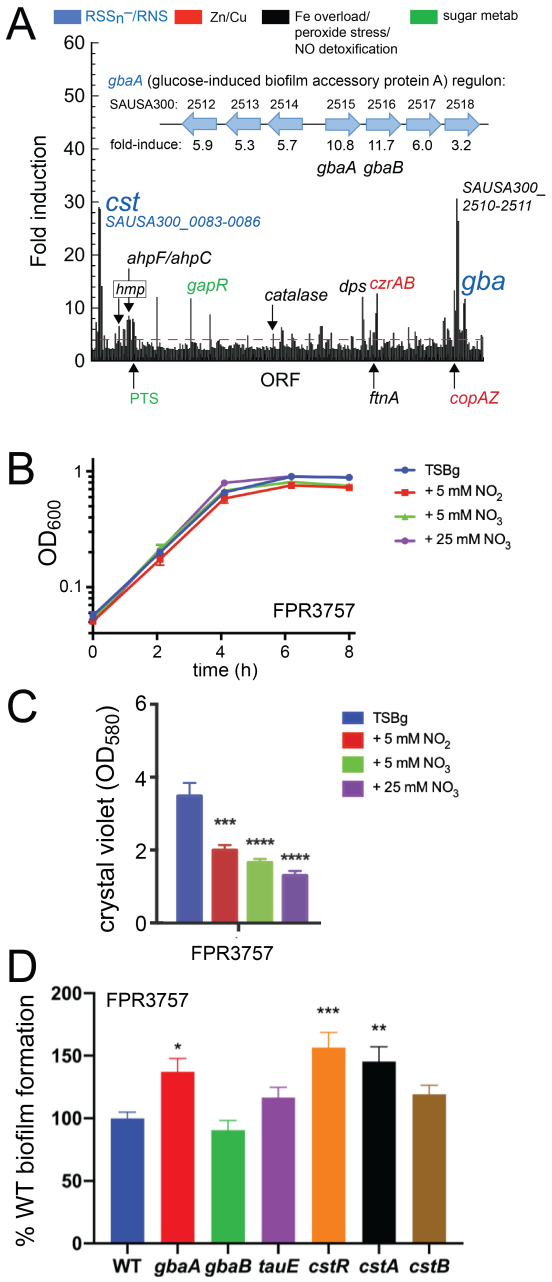

Figure S2. GbaA plays a role in the biofilm dynamics in MRSA strains**.** (A) Summary of the published results of a microarray-derived transcriptomics analysis of a nitrate-respiring *S. aureus* N315 biofilm stressed with nitrite (NO_2^-) (Fig. 3A).[1] Nitrate (NO_3^-) is a preferred host-derived electron acceptor for anaerobic respiration.[2] These conditions result in nitric oxide (NO)[3]-mediated *dispersal* of the N315 biofilm[4] and strong induction of the *cst* operon (SAUSA300_0083-0086, encoding TauE, CstR, CstA and CstB, respectively) characterized later,[5] along with NO (*hmp*),[6] ROS, Fe (*dps, ftnA*), Cu (*copAZ*)[7] and Zn (*czrAB*)[8,9]-resistance systems, as well as the regulon (*gba*) regulated by the tetracycline repressor (TetR)-family[10]

protein, glucose-induced biofilm accessory protein A (GbaA),[11,12] which is the subject of the work presented here. (B) Planktonic growth curves for the parent *S. aureus* USA300 FPR3757 strain used in these studies under conditions of NO_2^- and NO_3^- mediated biofilm dispersal in a TSB growth medium supplemented with 1% glucose (final) + 3% NaCl (final) (TSBg). (C) NO_2^- and NO_3^- mediated dispersal of *S. aureus* USA300 FPR3757 biofilms following two days growth at 37 ºC without shaking, washed 2X with PBS, prior to fixing and straining with crystal violet. (D) Biofilm yields plotted as % wild-type yield obtained following a 2-day incubation in TSBg with various FPR3757 strains: USA300 FPR3757 (WT), and insertionally inactivated *gbaA*, *gbaB*, *tauE*, *cstR*, *cstA* and *cstB* (**Table S1**). The *gbaA* FPR3757 strain gives rise to higher biofilm yields in a manner that appears dependent on *gbaB*, consistent with prior characterization of clinically isolated super-biofilm-elaborating *S. aureus* strains that encode a prematurely terminated *gbaA* allele.[11,12] Unregulated expression of the *cst* operon[5] also significantly impacts biofilm yields, consistent with the data in panel A. The results of biological quadruplicates and technical triplicates are shown in panels B-D (*, $p<0.05$; **, $p<0.01$; $p<0.005$).

Figure S3

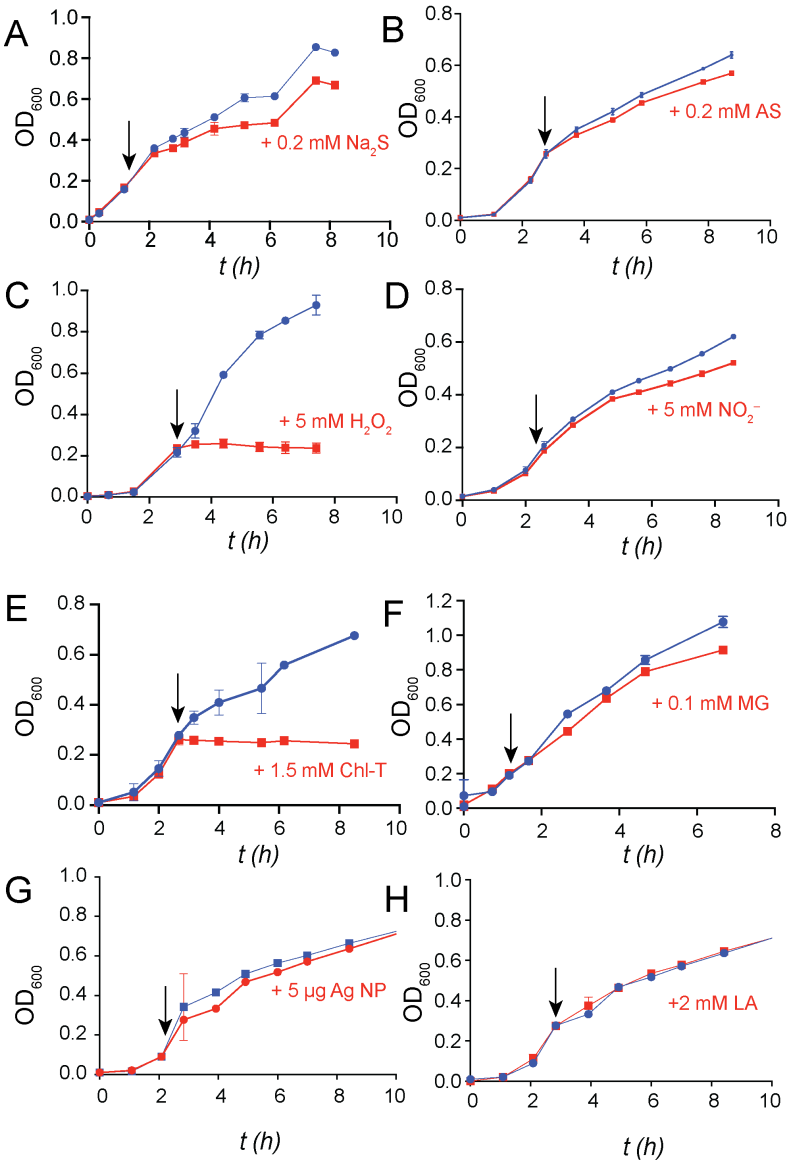

Figure S3. Growth curves for WT *S. aureus* FPR3757 with various stressors. WT *S. aureus* was grown aerobically with vigorous shaking at 37 ˚C without any stress (*blue* line) versus (A) 0.2 mM Na_2S[13], (B) 0.2 mM Angeli's salt (AS)[14], (C) 5 mM H_2O_2[15], (D) 5 mM $NaNO_2$ (nitrite)[1], (E) 1.5 mM Chloramine-T (Chl-T)[16], (F) 0.1 mM methyl glyoxal (MG)[16,17], (G) 5 µg Ag Nanoparticles (Ag NP)[18] and (H) 2 mM linoleic acid (LA)[19] added to the growing cells at mid-log phase (OD_{600} ≈0.2) (*red* line). Point of addition is marked by the *black* arrow. 5 mL of cells were collected 15 min following addition of the indicated reagent and worked up for qRT-PCR experiment (**Figure 2**, main text). The results of triplicate growth curves were averaged and the mean OD_{600} and standard deviation of the mean are shown.

Figure S4

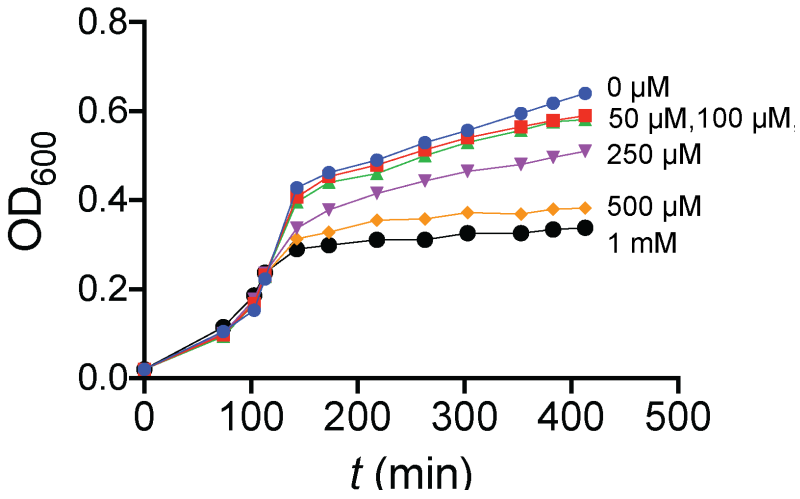

Figure S4. Dose-dependent growth curves of WT *S. aureus* USA300 FPR3757 exposed to the indicated concentrations of methylglyoxal (MG), added to mid-log cultures at an OD_{600} ≈0.2.

Figure S5

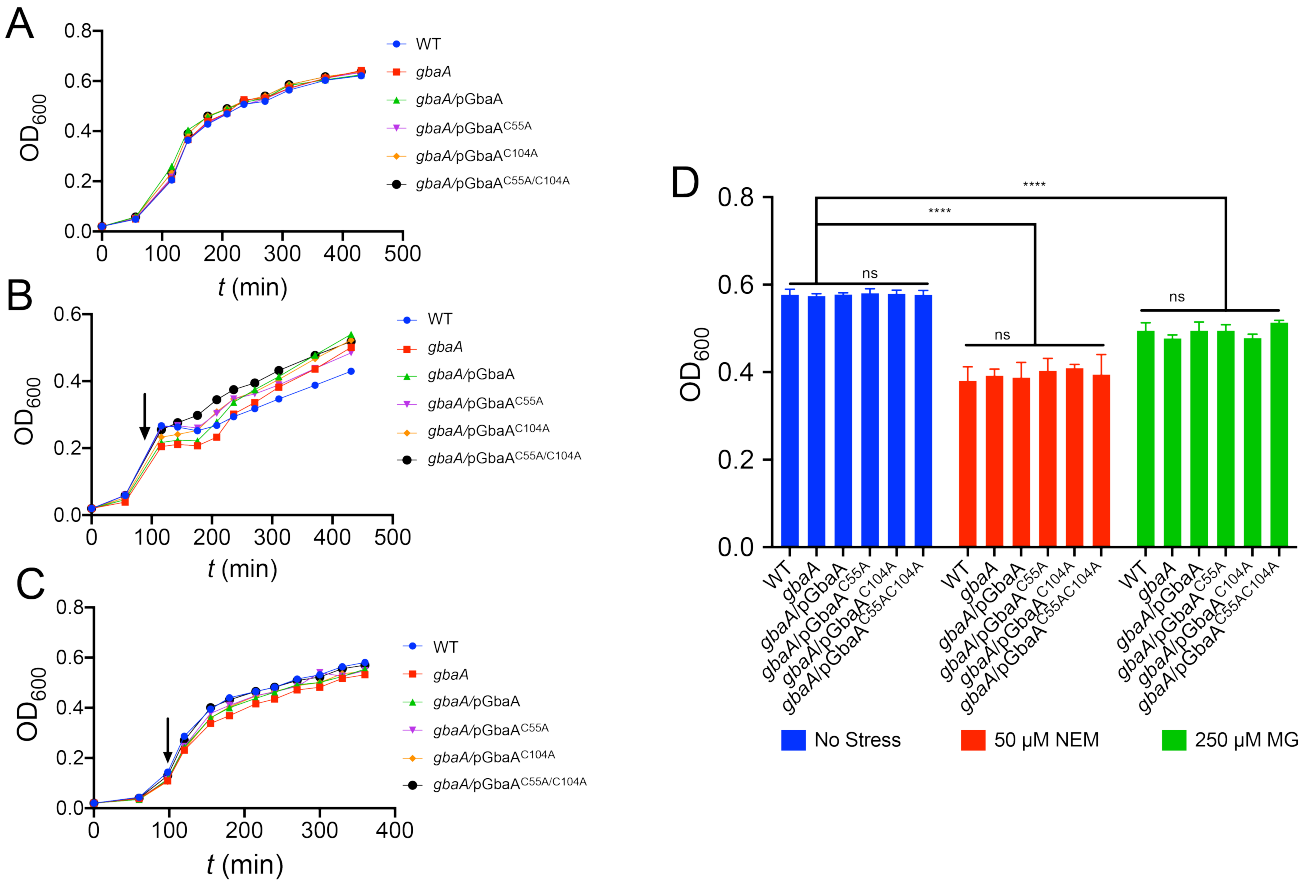

Figure S5. Representative growth curves that results upon addition of 50 μM NEM or 250 μM MG to *S. aureus* WT, *gbaA*, *gbaA*/pGbaA, *gbaA*/pGbaA^{C55A}, *gbaA*/pGbaA^{C104A}, *gbaA*/pGbaA^{C55AC104A} strains as indicated in the legend. (A) No stress added; (B) 50 μM NEM (sub-inhibitory concentration) added at the time point denoted by *black* arrow;(C) 250 μM MG (sub-inhibitory concentration) added at the time point denoted by *black* arrow; and (D) Average growth yields at t=305 ± 5 min for all the strains are shown for no stress (*blue* bars), 50 μM NEM (*red* bars) and 250 μM MG (*green* bars), while stressing the cells at an OD_{600} of 0.2. These experiments show the results of biological triplicates with statistical significance calculated using Student's paired T test (ns, not significant, *, p<0.05; **, p<0.01; ***,p<0.001; ****, p<0.0001). All *gbaA* strains exhibit growth yields that are indistinguishable from the that of the WT strain.

Figure S6

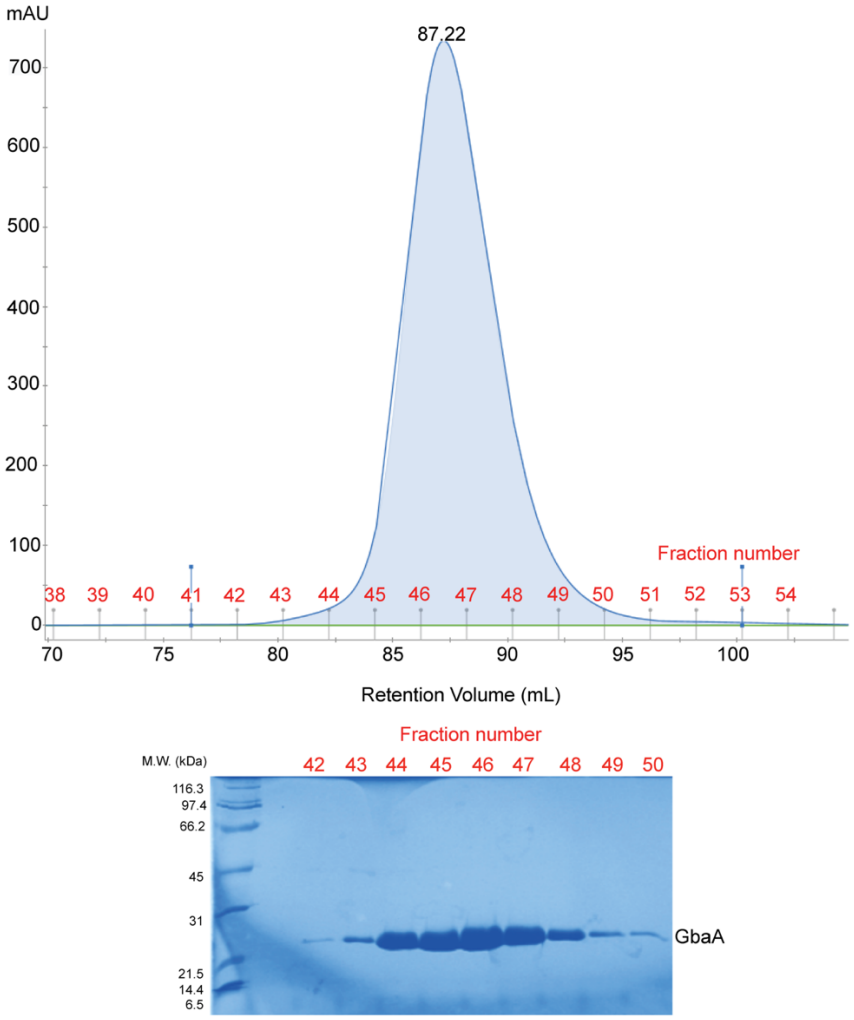

Figure S6. Representative final step of the purification of *S. aureus* GbaA. A preparative G75 column was used for size exclusion chromatography of GbaA (*top*) chromatogram showing the peak for GbaA appearing at the elution volume 87.2 mL, with 2 mL fractions (labeled in *red* text) collected and assayed for purity by SDS-PAGE analysis (bottom). Expected molecular weight is 22,186 kDa, with the observed molecular weight by ESI-MS of 22,186.0 kDa. Each GbaA preparation contained ≥1.82 thiols per monomer (≥91% thiol content) as quantified by the DTNB assay.[20]

Figure S7

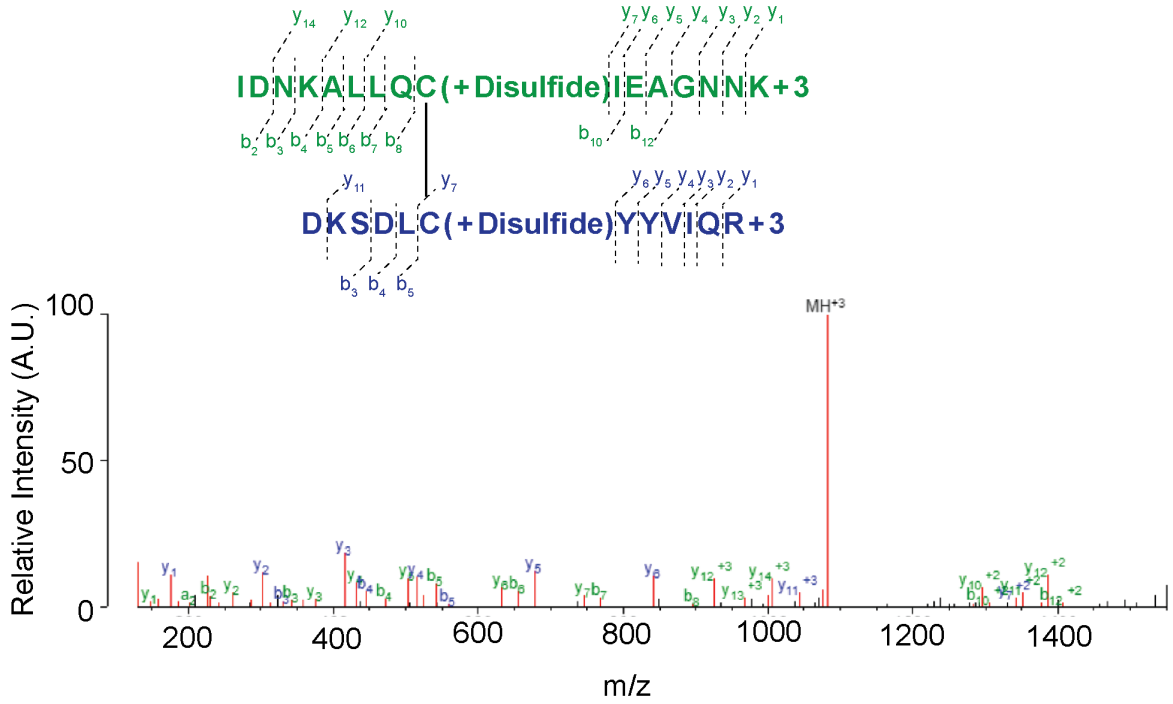

Figure S7. Tandem MS/MS data for disulfide oxidized GbaA. The trypsin-digested, diamide oxidized GbaA (see **Figure 3**, main text) was subjected to ESI-MS/MS with the fragmentation of the z=2 and z=3 charge states shown for a parent ion (MH^{+3}) suspected to contain the C55-C104 disulfide bond. b_i are N-terminally truncated fragment ions, y_i are C-terminally truncated fragment ions. The fragment ions observed in the MS/MS spectrum are labeled and correspond to those fragments indicated in the schematic at *top*, and provide direct evidence for a C55-C104 disulfide bond in oxidized GbaA.

Figure S8

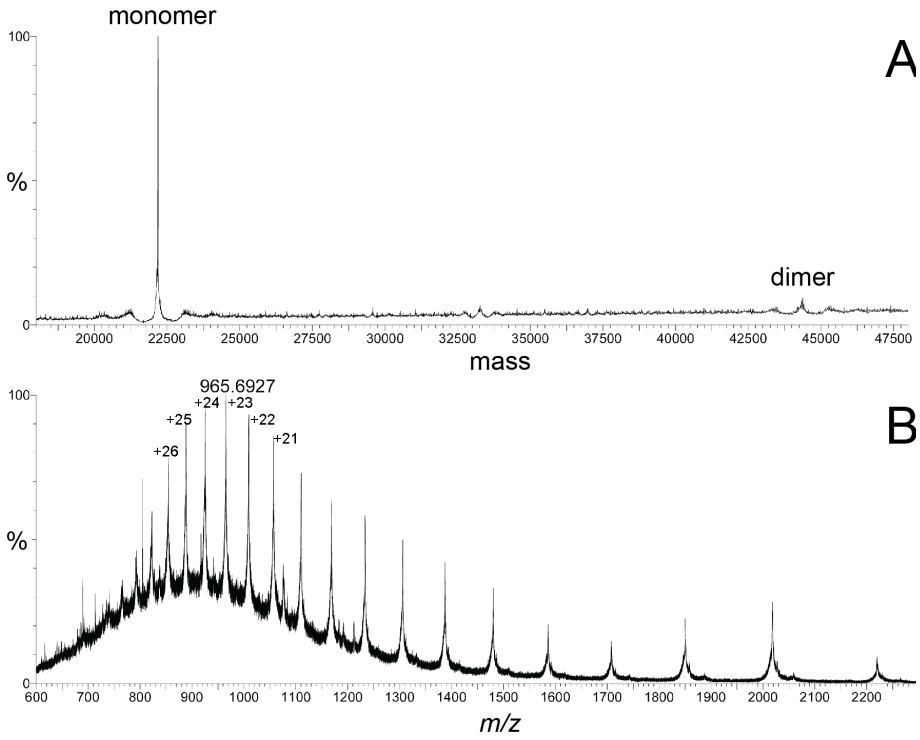

Figure S8. Charge-state deconvoluted (A) and raw (B) ESI-MS spectra of WT GbaA oxidized with GSSG. Wild-type GbaA was incubated overnight with 20-fold molar protomer excess of GSSG in an anaerobic atmosphere and free thiol content was quantified to be ≈10% by the DTNB assay. The expected mass for an oxidized GbaA monomer is 22,184 Da (see Figure 5A) 22,187 Da observed). The small fraction of dimer peak (44,374 Da observed) in this nearly quantitatively oxidized GbaA homodimer is consistent with an *intra*protomer G55–C104 crosslink as the major crosslinked species, with the crosslink confirmed by experiment shown in **Figure 3**, main text. Reaction conditions: 25 mM Tris buffer, 0.5 M NaCl, pH 7.5, ambient temperature.

Figure S9

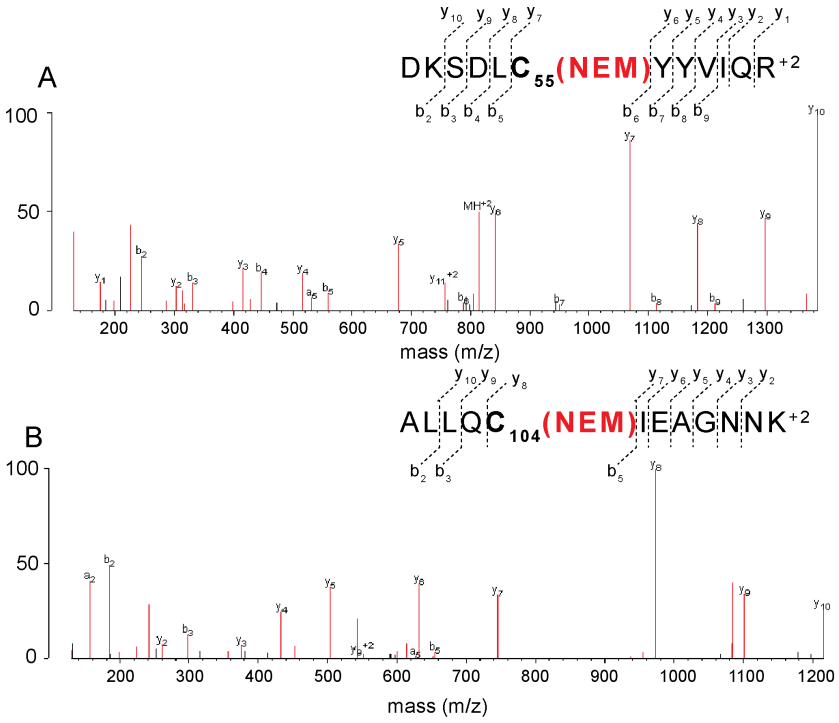

Figure S9. ESI-MS/MS spectra obtained for *N*-ethylmaleimide (NEM)-modified WT GbaA derived for the (A) C55-SNEM and (B) C104-SNEM derivatized peptides. Wild-type GbaA was incubated with NEM for 10 min and the protein washed and subjected to trypsin digestion followed by ESI-MS/MS. Fragmentation of the z=2 charge state is shown for the parent ion (MH^{+2}) for each peptide. b_i are N-terminally truncated fragment ions, y_i are C-terminally truncated fragment ions. The fragment ions observed in the MS/MS spectra are labeled in the cartoon, *inset*. Conditions: 25 mM Tris-HCl, 0.5 M NaCl, pH 7.5.

Figure S10

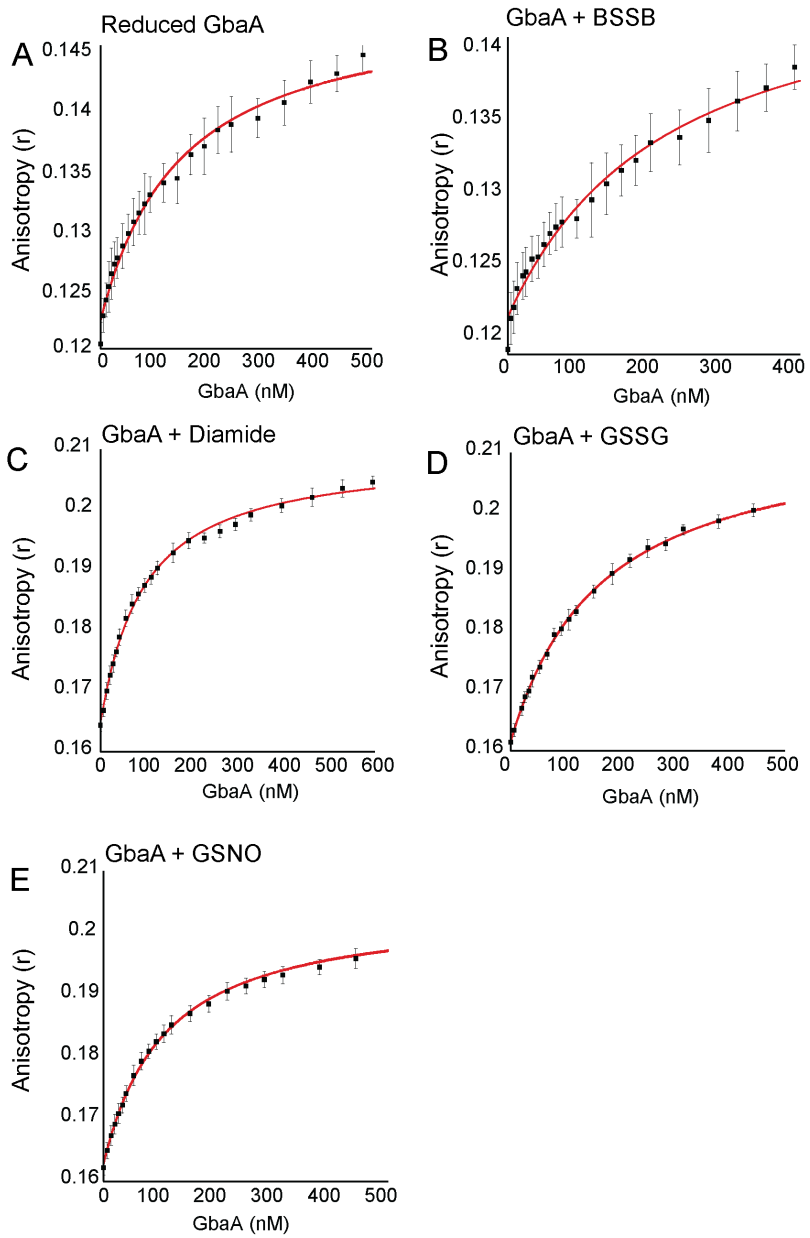

Figure S10. Representative fluorescence anisotropy (*r*)-based DNA binding experiments obtained for reduced and oxidized GbaA with GbaO operator (see Materials and Methods for operator sequence). (A) reduced GbaA; (B) Bacillithiol disulfide (BSSB)-oxidized GbaA; (C) Diamide (*N*,*N*,*N*′,*N*′-tetramethylazodicarboxamide)-oxidized GbaA; (D) Glutathione disulfide (GSSG)-oxidized GbaA; (E) *S*-nitrosoglutathione (GSNO)-oxidized GbaA. The DNA-binding affinities, K_a from at least duplicate experiments are shown in **Table 2**, main text. All oxidants shown here give rise to more than 87% oxidized (measured by the DTNB assay)[20] GbaA protomers and estimated by MALDI-MS (see **Figure 3**, main text) and confirmed by ESI-MS/MS (see **Figure S7**).

Figure S11

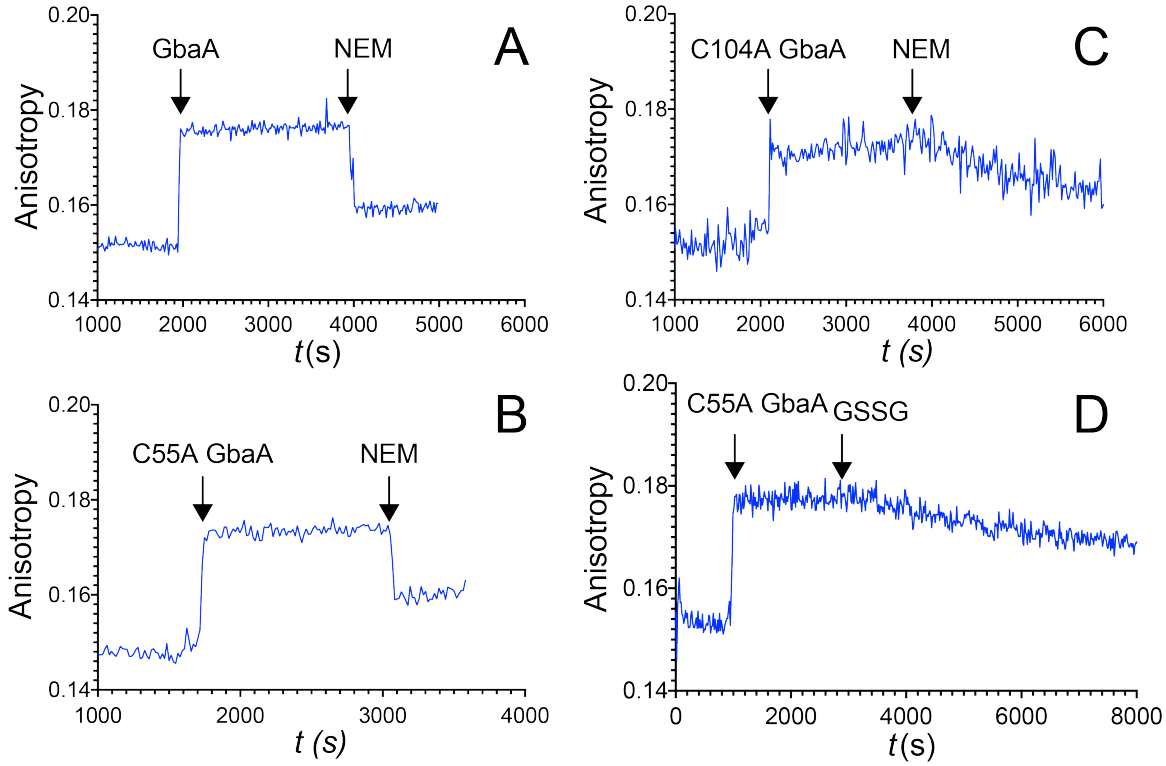

Figure S11. Monitoring the kinetics of the GbaA-DNA complex dissociation by NEM or GSSG. Reduced GbaA (100-150 nM protomer; to reach ≈50% saturation of the operator) was added to free OP1 DNA (10 nM) at the time point indicated by the left-most arrow and then NEM or GSSG was added to the complex at time point as indicated by the right-most arrow. (A) WT GbaA (100 nM)-DNA complex dissociated with 1 mM NEM; (B) C55A GbaA (100 nM) dissociated with 1 mM NEM; (C) C104A GbaA (150 nM) dissociated with 1 mM NEM; and (D) C55A GbaA (100 nM) dissociated with 1 mM GSSG. Conditions: 25 mM Tris-HCl, pH 7.5, 0.5 M NaCl.

Table S1. Strains, primers and DNA oligonucleotides used in this study. All strains are derived from *S. aureus* USA300 FPR3757

Strains	**Description**	**Reference**
WT *S. aureus*	*Staphylococcus aureus* USA300 FPR3757	(1)
gbaA	*SAUSA300_2515*::Tn(erm)	This study
gbaB	*SAUSA300_2516*::Tn(erm)	This study
tauE	*SAUSA300_0083*::Tn(erm)	This study
cstR	*SAUSA300_0084*::Tn(erm)	This study
cstA	*SAUSA300_0085*::Tn(erm)	This study
cstB	*SAUSA300_0086*::Tn(erm)	This study
Plasmids	**Description; use**	
pHIS	IPTG inducible T7 promoter, ampicillin resistance; protein purification	This study
pOS1	Constitutive promoter, ampicillin resistance for *E. coli,* CAM resistance for *Staphylococcus aureus*; complementation plasmids	
qRT-PCR primers	**Sequence (5'→3')**	**Amplicon Size (bp)**
duf2316 forward	CGCATCACAGCTGAAGAGTT	223 bp
duf2316 reverse	CTGGTGTTTGTCCATTTCCTTTAAT	
gbaB forward	CACCTCGTGACGTTGAAGAA	216 bp
gbaB reverse	GCATTGTTACTGCCGATTTAGAC	
GbaA purification	**Sequence (5'→3')**	
gbaApHis forward	AACCTGTATTTTCAGGGCGCCATGATGCGAAAAGATGCAAAAGAGAATAG	558 bp
gbaApHis reverse	TTAGTCATTACGTCCCACCTCATCTAAATATAAGAATTCAAAGGCCTACGTCGAC	
GbaA Complementation Sequence (5'→3')		
gbaApos1 forward	ATACAATTGAGGTGAACATATGCGAAAAGATGCAAAAGAGAATAGGCAAC	558 bp
gbaApos1 reverse	AACACTACCCCCTTGTTTGGATCCTTAGTCATTACGTCCCACCTCATCT	
Fluorescence Anisotropy experiments Sequence (5'→3')		
GbaO* forward[a]	TATAATAAACGGAGAGTTATCCGTTTGTCAA/3FluorT/	32 bp
GbaO reverse	ATTGACAAACGGATAACTCTCCGTTTATTATA	
CstO* forward	/5FluorT/ACCTCCAAATATACCCTTATGGGGTATATTAAA	34 bp
CstO reverse	TTTAATATACCCCATAAGGGTATATTTGGAGGTA	

[a]The sequence for the GbaO DNA operator was elucidated in earlier experiments by Yu *et al*.[11]

Table S2. Hydrodynamic parameters for reduced and oxidized GbaA as determined by small angle x-ray scattering (SAXS)[a]

SAXS parameter	Reduced GbaA	Oxidized GbaA
R_g (Å) (Guinier)	25.67	25.60
R_g (Å) (GNOM)	25.26	25.52
D_{max} (Å)	83.42	82.39
MW (Da)	48114	48379
MW discrepancy (%)	±8.4	±8.9
Oligomeric assembly state	Dimer	Dimer

[a]Buffer conditions: 25 mM Tris-HCl, pH 8.0, 0.5 M NaCl with and without 0.5 mM TCEP for reduced and oxidized proteins, respectively.

Table S3. Peptides observed in a trypsin-digested NEM-treated wild-type GbaA detected as a variable modification by LC-ESI-MS/MS.[a]

m/z	*z*	ppm	DB Peptide	Variable Modification
553.8013	2	-0.018	**Q**RIEEIAHK	Gln to pyro-Glu at 1
281.6608	4	-0.3	QRIEEIAHK	
420.2346	2	-0.21	IEEIAHK	
834.8801	2	-0.24	LFDEEGVENIS**M**NR	Oxidation at 12
551.5903	3	-1.2	LFDEEGVENISMNR	
513.2847	3	-0.68	IAKELGIG**M**GTLYR	Oxidation at 9
507.9533	3	-0.37	IAKELGIGMGTLYR	
613.3157	2	-0.29	ELGIG**M**GTLYR	Oxidation at 6
605.3176	2	-1.4	ELGIGMGTLYR	
814.3934	2	0.61	DKSDL**C**YYVIQR **(C55)**	***N*-ethylmaleimide at 6**
751.8691	2	0.14	DKSDLCYYVIQR	
692.832	2	0.073	SDL**C**YYVIQR **(C55)**	***N*-ethylmaleimide at 4**
420.5412	3	0.058	SDLCYYVIQR	
416.8923	3	-0.035	DLDIFITHFK	
992.476	3	0.11	**Q**IKDDYHSNYEV**M**QVSLDYLLQFK	Gln to pyro-Glu at 1 Oxidation at 13
987.1452	3	0.95	**Q**IKDDYHSNYEVMQVSLDYLLQFK	Gln to pyro-Glu at 1
1496.724	2	0.095	QIKDDYHSNYEV**M**QVSLDYLLQFK	Oxidation at 13
992.8172	3	-2.6	QIKDDYHSNYEVMQVSLDYLLQFK	
875.0728	3	0.68	DDYHSNYEV**M**QVSLDYLLQFK	Oxidation at 10
699.8565	2	0.83	ALLQ**C**IEAGNNK **(C104)**	***N*-ethylmaleimide at 5**
637.3319	2	-0.37	ALLQCIEAGNNK	
771.9237	2	-1.3	ALLQCIEAGNNKLR	
845.391	3	-0.2	FYQSAFYQELFDFYYDLFK	
872.1169	3	1	FKTD**M**LLQSLSTSVFAFQIEHR	Oxidation at 5
866.7851	3	0.88	FKTDMLLQSLSTSVFAFQIEHR	
1170.089	2	0.61	TD**M**LLQSLSTSVFAFQIEHR	Oxidation at 3
775.0636	3	0.5	TDMLLQSLSTSVFAFQIEHR	
330.1785	3	-0.11	HISIEAYR	
851.1147	3	-0.33	HISIEAYRNYLLNIYLDEVGR	
527.9473	3	0.078	NYLLNIYLDEVGR	
604.3051	3	2.1	NYLLNIYLDEVGRND	

[a]C55 and C104 *S*-alkylated peptides (SNEM) are highlighted in *bold*.

Supplementary References

[1] Schlag, S., Nerz, C., Birkenstock, T. A., Altenberend, F., and Götz, F. (2007) Inhibition of Staphylococcal Biofilm Formation by Nitrite, *J Bacteriol 189*, 7911-7919.

[2] Winter, S. E., Winter, M. G., Xavier, M. N., Thiennimitr, P., Poon, V., Keestra, A. M., Laughlin, R. C., Gomez, G., Wu, J., Lawhon, S. D., Popova, I. E., Parikh, S. J., Adams, L. G., Tsolis, R. M., Stewart, V. J., and Baumler, A. J. (2013) Host-derived nitrate boosts growth of *E. coli* in the inflamed gut, *Science 339*, 708-711.

[3] Tiso, M., and Schechter, A. N. (2015) Nitrate Reduction to Nitrite, Nitric Oxide and Ammonia by Gut Bacteria under Physiological Conditions, *PLoS One 10*, e0119712.

[4] Barraud, N., Kelso, M. J., Rice, S. A., and Kjelleberg, S. (2015) Nitric Oxide: a Key Mediator of Biofilm Dispersal with Applications in Infectious Diseases, *Curr Pharm Des*. *21*, 31-42.

[5] Luebke, J. L., Shen, J., Bruce, K. E., Kehl-Fie, T. E., Peng, H., Skaar, E. P., and Giedroc, D. P. (2014) The CsoR-like sulfurtransferase repressor (CstR) is a persulfide sensor in *Staphylococcus aureus, Mol Microbiol 94*, 1343-1360.

[6] Richardson, A. R., Libby, S. J., and Fang, F. C. (2008) A nitric oxide-inducible lactate dehydrogenase enables *Staphylococcus aureus t*o resist innate immunity, *Science 319*, 1672-1676.

[7] Djoko, K. Y., Franiek, J. A., Edwards, J. L., Falsetta, M. L., Kidd, S. P., Potter, A. J., Chen, N. H., Apicella, M. A., Jennings, M. P., and McEwan, A. G. (2012) Phenotypic characterization of a *copA* mutant of *Neisseria gonorrhoeae* identifies a link between copper and nitrosative stress, *Infect Immun 80*, 1065-1071.

[8] Kuroda, M., Hayashi, H., and Ohta, T. (1999) Chromosome-determined zinc-responsible operon *czr* in *Staphylococcus aureus* strain 912, *Microbiol Immunol 43*, 115-125.

[9] Eicken, C., Pennella, M. A., Chen, X., Koshlap, K. M., VanZile, M. L., Sacchettini, J. C., and Giedroc, D. P. (2003) A Metal–Ligand-mediated Intersubunit Allosteric Switch in Related SmtB/ArsR Zinc Sensor Proteins, *J Mol Biol 333*, 683-695.

[10] Cuthbertson, L., and Nodwell, J. R. (2013) The TetR family of regulators, *Microbiol Mol Biol Rev 77*, 440-475.

[11] Yu, L., Hisatsune, J., Hayashi, I., Tatsukawa, N., Sato'o, Y., Mizumachi, E., Kato, F., Hirakawa, H., Pier, G. B., and Sugai, M. (2017) A Novel Repressor of the ica Locus Discovered in Clinically Isolated Super-Biofilm-Elaborating *Staphylococcus aureus*, *mBio 8*, e02282-16.

[12] You, Y., Xue, T., Cao, L., Zhao, L., Sun, H., and Sun, B. (2014) *Staphylococcus aureus* glucose-induced biofilm accessory proteins, GbaAB, influence biofilm formation in a PIA-dependent manner, *Int J Med Microbiol 304*, 603-612.

[13] Peng, H., Zhang, Y., Palmer, L. D., Kehl-Fie, T. E., Skaar, E. P., Trinidad, J. C., and Giedroc, D. P. (2017) Hydrogen Sulfide and Reactive Sulfur Species Impact Proteome *S*-Sulfhydration and Global Virulence Regulation in *Staphylococcus aureus*, *ACS Infect Dis 3*, 744-755.

[14] Shen, J., Walsh, B. J. C., Flores-Mireles, A. L., Peng, H., Zhang, Y., Zhang, Y., Trinidad, J. C., Hultgren, S. J., and Giedroc, D. P. (2018) Hydrogen Sulfide Sensing through Reactive Sulfur Species (RSS) and Nitroxyl (HNO) in *Enterococcus faecalis*, *ACS Chem Biol 13*, 1610-1620.

[15] Antelmann, H., Engelmann, S., Schmid, R., and Hecker, M. (1996) General and oxidative stress responses in *Bacillus subtilis*: cloning, expression, and mutation of the alkyl hydroperoxide reductase operon, *J Bacteriol 178*, 6571-6578.
[16] Gray, M. J., Wholey, W. Y., Parker, B. W., Kim, M., and Jakob, U. (2013) NemR is a bleach-sensing transcription factor, *J Biol Chem 288*, 13789-13798.
[17] Subhadra, B., Surendran, S., Kim, D. H., Woo, K., Oh, M. H., and Choi, C. H. (2019) The transcription factor NemR is an electrophile-sensing regulator important for the detoxification of reactive electrophiles in *Acinetobacter nosocomialis*, *Res Microbiol 170*, 123-130.
[18] Wang, J., Li, J., Guo, G., Wang, Q., Tang, J., Zhao, Y., Qin, H., Wahafu, T., Shen, H., Liu, X., and Zhang, X. (2016) Silver-nanoparticles-modified biomaterial surface resistant to *Staphylococcus*: New insight into the antimicrobial action of silver, *Sci Rep 6*, 32699.
[19] Kenny, J. G., Ward, D., Josefsson, E., Jonsson, I. M., Hinds, J., Rees, H. H., Lindsay, J. A., Tarkowski, A., and Horsburgh, M. J. (2009) The *Staphylococcus aureus* response to unsaturated long chain free fatty acids: Survival mechanisms and virulence implications, *PLoS One 4*, e4344.
[20] Ellman, G. L., Courtney, K. D., Andres, V., Jr., and Feather-Stone, R. M. (1961) A new and rapid colorimetric determination of acetylcholinesterase activity, *Biochem Pharmacol 7*, 88-95.